Exciton Lifetime Paradoxically Enhanced by Dissipation and Decoherence: Toward Efficient Energy Conversion of a Solar Cell

Yasuhiro Yamada,[1,*] Youhei Yamaji,[2] and Masatoshi Imada[1]
[1]Department of Applied Physics, The University of Tokyo, 7-3-1 Hongo, Bunkyo-ku, Tokyo 113-8656, Japan
[2]Quantum-Phase Electronics Center (QPEC), The University of Tokyo, 7-3-1 Hongo, Bunkyo-ku, Tokyo 113-8656, Japan
(Received 13 February 2015; published 6 November 2015)

Energy dissipation and decoherence are at first glance harmful to acquiring the long exciton lifetime desired for efficient photovoltaics. In the presence of both optically forbidden (namely, dark) and allowed (bright) excitons, however, they can be instrumental, as suggested in photosynthesis. By simulating the quantum dynamics of exciton relaxations, we show that the optimized decoherence that imposes a quantum-to-classical crossover with the dissipation realizes a dramatically longer lifetime. In an example of a carbon nanotube, the exciton lifetime increases by nearly 2 orders of magnitude when the crossover triggers a stable high population in the dark excitons.

DOI: 10.1103/PhysRevLett.115.197701 PACS numbers: 84.60.-h, 42.50.Ct, 78.67.Ch

Sunlight is a clean, abundant, and sustainable energy source. Hence, effective energy conversion from sunlight into electricity is a grand challenge in science and technology, which leads to an emerging interest in post-silicon photovoltaic materials such as carbon nanotubes, quantum dots, and transition metal dichalcogenides for their promising applications [1–3]. Energy conversion consists of three processes of nonequilibrium quantum dynamics of excitons (bound electron-hole pairs): exciton generation from a photon, exciton energy transfer, and charge separation of the exciton into electrodes. In the first two processes, efficient conversion requires both a high photon absorption rate and long exciton lifetime. However, optimization is hampered by the reversibility between the absorption and emission of a photon in quantum dynamics: while a high absorption rate for the photon is desired in the exciton generation process, it also leads to a high charge recombination rate for the exciton.

In this work, we show that a desired remarkable enhancement of the exciton lifetime by simultaneously keeping a high absorption rate is achieved by utilizing nonequilibrium energy dissipation and decoherence by phonons. Though dissipation is in general an obstacle to a high efficiency of energy conversion, there are cases where nonequilibrium dissipations and decoherence are actually instrumental in achieving a long exciton lifetime because they can suppress the exciton recombination by making quantum dynamics irreversible via a concomitant quantum-to-classical crossover [4].

In fact, irreversible exciton dynamics is exploited in photosynthesis that also includes the above mentioned three processes, namely, the exciton generation, the exciton energy transfer, and the charge separation [5,6]. Photosynthesis achieves a remarkably high quantum efficiency reaching nearly 100% [7], which means that an absorbed photon is converted to an exciton with no recombination. In the exciton generation process, the absorbed energy is irreversibly transferred from the optically allowed bright exciton to an optically forbidden dark exciton [8–10], which can act as a ratchet between the exciton generation process and the next energy transfer process where the quantum coherence plays a role again [11–15].

Recently, photovoltaic models inspired by photosynthesis were studied from the viewpoint of steady-state heat engines modified with discrete exciton states [16–18]. A mechanism for the enhancement of the photocurrent was proposed by designing the ultrafast classical transition from bright to dark excitons within a hundred femtoseconds, where quantum coherence between photons and excitons and the resultant photoluminescence causing the recombination were also ignored [17]. However, these classical descriptions of the photocell dynamics make the validity of the enhancement questionable because the inherent dichotomy between quantum coherence and decoherence is a crucial issue in enhancing quantum efficiency in the target time domain: on the one hand, the desired ultrafast transition from the bright to the dark excitons necessarily requires quantum coherent dynamics, whereas, on the other hand, the decoherence that imposes a quantum-to-classical crossover is assumed to immediately occur.

For the microscopic understanding of optimal energy conversions, here we study the transient dynamics for the exciton generation process, taking account of the dichotomy in a unified quantum manner. To this end, we construct and investigate an open quantum model that consists of bright and dark excitons coupled with phonons and a dissipative photon, using the combined method of the generalized quantum master equation (GQME) [19] and the quantum continuous measurement theory of photon counting [20,21]. We found that the realistic coexistence of coherence and decoherence is the key for high quantum efficiency of photovoltaics. The crossover from quantum to classical dynamics due to dissipation and decoherence by phonons assists the long exciton lifetime: rapid quantum energy transfer from the bright to dark excitons suppresses the

initial radiative loss, whereas the dark excitons become stable through the concomitant crossover. Our results indeed reveal why the high efficiency of exciton generation from photons can be compatible with the low photoluminescence by violating the reversibility as observed experimentally.

By taking a typical semiconducting single-walled carbon nanotube (SWCNT) with (6,5) chirality as a model material, we demonstrate that the exciton lifetime becomes nearly 2 orders of magnitude longer than in the case without dark excitons. In the SWCNT, at least two dark exciton states exist with energy below the lowest bright one [22–38]: the even-parity dark exciton [22,23,33,34] and the spin-triplet dark exciton [24,25,35,36]. Because the lower dark states can pave the way for the relaxation of the bright one by harnessing the environmental dissipation and decoherence, we construct a Hamiltonian consisting of one bright and two dark exciton states coupled to a phonon continuum and a single photon [39] (see Fig. 1), as a minimal model of the exciton generation in the (6,5) SWCNT that accounts for the substantial photon absorption at the bright exciton level separated from the band gap [40–42] and the characteristic photoluminescence with multiexponential decay [22,23,25,43,44] and low quantum yields [45].

The model Hamiltonian is given by

$$\hat{H} = \hat{H}_S + \hat{H}_B + \hat{H}_{\rm Int}. \tag{1}$$

The first term is the Hamiltonian of the exciton-photon system $\hat{H}_S = \hbar\omega_{\rm ph}\hat{a}^\dagger\hat{a} + \sum_{r={\rm br},d1,d2}\varepsilon_r\hat{b}_r^\dagger\hat{b}_r + \hbar g(\hat{b}_{\rm br}^\dagger\hat{a} + \hat{a}^\dagger\hat{b}_{\rm br})$ with $\hat{a}^\dagger$, $\hat{b}_{\rm br}^\dagger$, and $\hat{b}_{d1,d2}^\dagger$ being the bosonic creation operators for the photon, the bright exciton, and the two dark excitons (dark 1 and dark 2), respectively, where the dark-1 (dark-2) exciton has even-parity (triplet) symmetry. The bright exciton is coupled to the photon with the dipole coupling strength g. The second term represents the phononic bath $\hat{H}_B = \sum_{r=d1,d2}\sum_{\boldsymbol{q}}\hbar\Omega_{r\boldsymbol{q}}\hat{p}_{r\boldsymbol{q}}^\dagger\hat{p}_{r\boldsymbol{q}}$, where $\hat{p}_{r\boldsymbol{q}}^\dagger$ reads the bosonic creation operator of a phonon with momentum $\boldsymbol{q}$. The energies of the photon, the excitons, and the phonons are represented by $\hbar\omega_{\rm ph}$, $\varepsilon_{r=d1,d2}$, and $\hbar\Omega_{r\boldsymbol{q}}$, respectively. The last term indicates the phonon-mediated coupling between the bright and dark excitons

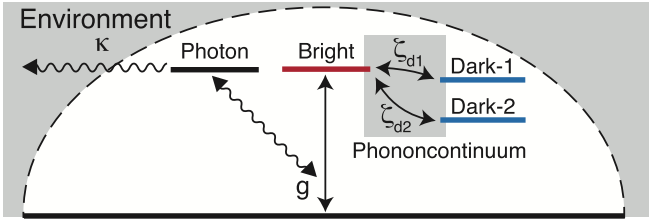

FIG. 1 (color online). Dissipative quantum model of excitons in a semiconducting single-walled carbon nanotube with (6,5) chirality. Both the bright exciton generation and the charge recombination result from the dipole coupling with photons with the same strength g. The photons are dissipated to the environment with the rate κ. The bright exciton is coupled with two dark excitons via a phonon continuum.

$\hat{H}_{\rm Int} = \sum_{r=d1,d2}\sum_{\boldsymbol{q}}\hbar\zeta_{r\boldsymbol{q}}(\hat{b}_r^\dagger\hat{b}_{\rm br} + \hat{b}_{\rm br}^\dagger\hat{b}_r)(\hat{p}_{r\boldsymbol{q}}^\dagger + \hat{p}_{r\boldsymbol{q}})$ with the effective coupling strength $\zeta_{r\boldsymbol{q}}$.

Our Hamiltonian describes single photon absorption and luminescence processes, which is consistent with dilute, incoherent, and independent incoming photons in a single conversion cycle of nanoscale solar cells under the standard air mass (AM) 1.5 sunlight illumination [39]. In addition, here, the defect free model is employed to describe the pristine (6,5) SWCNT with low quantum yields and less defects [39,46,47] where the nonradiative multiphonon decay hardly affects the exciton relaxation up to $t > 1$ μs [39,48].

Simulating the radiative lifetime of excitons requires nonunitary dissipations of the photon to the environment or by photodetection. We simulate the nonunitary events by using the photon counting theory with the photon dissipation rate, $\kappa \geq 0$ [20,21]. The photon counting gives the probability that m photons are absorbed to environments (or disappear at the instrument) in the time interval $[0, t]$: $\mathcal{P}(m;t)$.

For feasible simulations of the excitons with photon counting, we use the moment generating function (MGF) of the probability, $\mathcal{M}(\lambda;t) \equiv \sum_{m=-\infty}^{\infty}\exp[im\lambda]\mathcal{P}(m;t)$ with the conjugate variable λ to m. The details of the formalism below are described in the Method section of the Supplemental Material [39] using dynamical maps [49–51] in Liouville space [52,53]. The MGF dynamics can be explicitly determined by the following equation of motion for a generalized density matrix with λ: $\partial_t\hat{\rho}(t;\lambda) = -i[\hat{H},\hat{\rho}(t;\lambda)]/\hbar + \kappa e^{i\lambda}\hat{a}\hat{\rho}(t;\lambda)\hat{a}^\dagger - \kappa[\hat{a}^\dagger\hat{a}\hat{\rho}(t;\lambda) + \hat{\rho}(t;\lambda)\hat{a}^\dagger\hat{a}]/2$, where the MGF is given by the trace of $\hat{\rho}(t;\lambda)$ as $\mathcal{M}(\lambda;t) = {\rm Tr}[\hat{\rho}(t;\lambda)]$ with $\hat{\rho}(t=0;\lambda) = \hat{\rho}_0$ being the initial density matrix just after the photon absorption at $t = 0$. Applying the Franck-Condon principle, $\hat{\rho}_0$ is reasonably given by $\hat{\rho}_0 \propto \hat{\rho}_0^S \otimes \exp[-\hat{H}_B/k_BT]$ where $\hat{\rho}_0^S$ is the one-bright-exciton state and T is the temperature of the phononic bath.

From now on, we assume that the coupling strength $\zeta_{r\boldsymbol{q}}$ is weak and take the influence into account by the standard second-order perturbation approximation in terms of $\hat{H}_{\rm Int}$ [19]. In this approximation, the exciton dynamics is adequately described by the GQME for the generalized reduced density matrix (RDM) $\hat{\rho}^S(t;\lambda) \equiv {\rm Tr}_B[\hat{\rho}(t;\lambda)]$, where ${\rm Tr}_B$ means the partial trace of the phononic bath, and the influence of the phonons on the exciton system is represented by the spectral density $J_r(\omega) \equiv \sum_{\boldsymbol{q}}|\zeta_{r\boldsymbol{q}}|^2\delta(\omega - \Omega_{r\boldsymbol{q}})$ for $r = d1, d2$. Here, we assume that $J_r(\omega)$ has the standard Ohmic form [19] $J_r(\omega) = 2\gamma_r^2\omega\theta(\omega_{\rm cut} - \omega)/\omega_{\rm cut}^2$ with $\gamma_r \equiv \sqrt{\sum_{\boldsymbol{q}}|\zeta_{r\boldsymbol{q}}|^2}$ and $\omega_{\rm cut}$ being the cutoff frequency of the spectral density, which well mimics the phonon density of states in SWCNTs after taking into account the thermal smearing at room temperature.

Solving the GQME numerically, we calculate the generalized RDM that gives the MGF as $\mathcal{M}(\lambda;t) = {\rm Tr}_S[\hat{\rho}^S(t;\lambda)]$. Note that the Markov dynamics emerges at the characteristic time proportional to the thermal relaxation time of the phonon bath $\tau_B \equiv \hbar/k_BT$ because the thermal

bath loses the memory of the system dynamics. See the Supplemental Material for the Markovian region [39]. The generalized RDM $\hat{\rho}^S(t;\lambda=0)$ coincides with the actual density matrix of the reduced system where we ignore the counting history, $\hat{\rho}^S(t)=\hat{\rho}^S(t;\lambda=0)$ [20,21,39]. Hereafter, we omit the script "S" representing the subspace of the exciton-photon system such as $\hat{\rho}^S(t)\to\hat{\rho}(t)$ for simplicity.

Actual time-resolved photoluminescence experiments have the time-resolution limit $\Delta\tau$, which is introduced phenomenologically by the Gaussian averaging: $\tilde{\mathcal{P}}(m,t)\equiv\frac{1}{\sqrt{2\pi}\Delta\tau}\int_{-\infty}^{\infty}\mathcal{P}(m,\tau)\exp[-(\tau-t)^2/(\sqrt{2}\Delta\tau)^2]d\tau$. From the time-averaged probability with $\Delta\tau=0.1$ ps, the time-resolved photoluminescence $L(t)\equiv\sum_m m\partial_t\tilde{\mathcal{P}}(m;t)$ and the quantum yield at a time t, $Y(t)\equiv\sum_m m\tilde{\mathcal{P}}(m;t)$ are calculated.

For a model calculation of (6,5) SWCNTs at room temperature, we choose the value of the parameters as follows: $\hbar\omega_{\rm ph}=\varepsilon_{\rm br}=1.27\,{\rm eV}$, $\varepsilon_{d1}=1.265\,{\rm eV}$, $\varepsilon_{d2}=1.15\,{\rm eV}$, $T=300$ K, $\hbar\omega_{\rm cut}=0.2$ eV, $\hbar g=10.5$ meV, $\hbar\gamma_{d1}=0.875$ meV, and $\hbar\gamma_{d2}=0.25$ meV. Since the environmental dissipation rate κ strongly depends on the ambient solvents, matrices, and/or substrates, we vary κ over several orders of magnitude. The energy levels of bright and dark excitons are estimated from the photoluminescence experiments [22,33–36]. The cutoff frequency of the spectral density $\hbar\omega_{\rm cut}$ is determined from the density of states of phonons in SWCNTs [54]. The coupling strength $\gamma_{d1,d2}$ is determined from the numerical fitting that reproduces the experiment [23] [see Fig. 3(c)]. The dipole coupling strength g is taken to be $g\gg\gamma_{d1,d2}$. Note that one confirms that 1 order of magnitude difference in g does not affect our main results.

First, we show the time-resolved photoluminescence $L(t)$ for $\kappa^{-1}=10$ ns in Fig. 2(a), which may be a typical result for SWCNTs in aqueous solutions. The simulated $L(t)$ is accurately fitted by a triexponential function:

$$L_{\rm fit}(t)=l_1e^{-t/\tau_1}+l_2e^{-t/\tau_2}+l_3e^{-t/\tau_3} \tag{2}$$

with $\tau_1<\tau_2<\tau_3$, which is consistent with the experiments [22,23,25,43,44]. The decay constants obtained in our calculation differ by several orders of magnitude: the fast decay is characterized by $\tau_1=65$ ps while the intermediate and slow decay constants τ_2 and τ_3 are found at 890 ps and 1 μs, respectively. Whereas the luminescence rapidly decreases within 1 ns, the quantum yields grow very slowly, which is also consistent with the experiments [22–25].

To characterize the relaxation dynamics, we define the exciton lifetime $\tau_{\rm LT}$ as the energy decay time to $1/e$ of the initial value for consistency with the single-exponential decay model:

$$E(\tau_{\rm LT})/E(0)\equiv e^{-1}. \tag{3}$$

From the definition, we obtain $\tau_{\rm LT}=880$ ns, which is longer than 40 times of that in the system with no dark exciton given by $\tau_{\rm LT}^{\rm nodark}=2\kappa^{-1}=20$ ns as detailed later. Here, the factor of '2" in $2\kappa^{-1}$ results from the halved residence time of the photon state by the Rabi oscillation between the photon and the bright exciton [55].

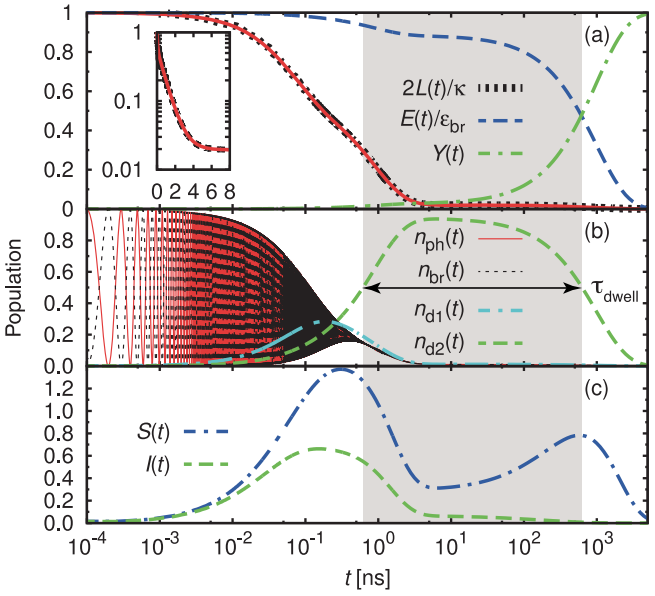

FIG. 2 (color online). (a) Time-resolved photoluminescence $L(t)$ and quantum yield $Y(t)$. The parameter for radiative dissipation to the environment is fixed at $\kappa^{-1}=10$ ns. The solid red line indicates the triexponential fitting of the numerical result $L_{\rm fit}(t)$. The time-dependent energy $E(t)\equiv{\rm Tr}[\hat{\rho}(t)\hat{H}_S]$ is also plotted in the same figure. (b) Population dynamics of the exciton-photon system with $n_{\rm ph}(t)\equiv{\rm Tr}[\hat{\rho}(t)\hat{a}^\dagger\hat{a}]$ and $n_{r={\rm br},d1,d2}(t)\equiv{\rm Tr}[\hat{\rho}(t)\hat{b}_r^\dagger\hat{b}_r]$. The shadow region indicates the dwell time $\tau_{\rm dwell}\approx630$ ns. (c) Time evolution of the von Neumann entropy $S(t)$ and the quantum mutual information $I(t)$.

The enhanced energy lifetime of the exciton-photon system is attributed to the fast irreversible relaxation pathway from the bright exciton to the dark excitons accompanied by the quantum-to-classical crossover as shown in Fig. 2(b). The initial dynamics has a quantum

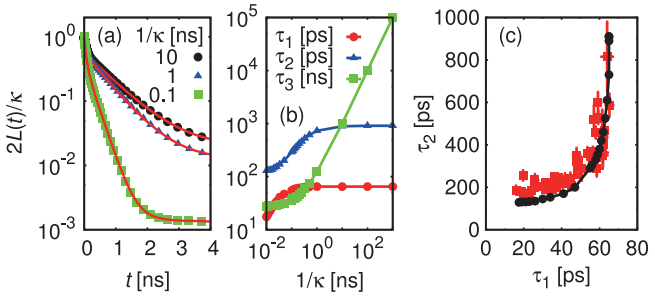

FIG. 3 (color online). (a) Time-resolved photoluminescence with several choices of κ^{-1}. The solid red lines indicate the triexponential fitting functions on the numerical results. (b) κ dependence of decay constants in the triexponential fitting function. (c) Correlation between τ_1 and τ_2 for several choices of κ^{-1} ranging from 10 ps to 1 μs (black filled circles). The filled square (red) symbols indicate the experimentally measured decay constants for the (6,5) SWCNT reproduced from Ref. [23].

nature where the populations of the photon and the bright exciton show Rabi oscillations with frequency $g/2$. Then, the population is gradually transferred to the dark excitons after 10 ps with a reduction of the oscillation due to decoherence effects by phonons. In particular, the population is stabilized at the dark-2 exciton with a long dwell time $\tau_{\rm dwell}$ defined by the time interval where the dark-2 exciton holds the population above 0.5. Note that the dark-1 exciton does not play an appreciable role in determining $\tau_{\rm dwell}$ as detailed in the Supplemental Material [39], whereas it is required to reproduce the triexponential decay of the photoluminescence observed in the experiments [23,25]. Indeed, the triexponential decay is ascribed to three different transient dynamics. Namely, the fast and the intermediate decays are attributed to the irreversible relaxation pathways from the bright exciton to the dark excitons and from the dark-1 exciton to the dark-2 exciton, respectively, while the slow one originates from the population decay from the whole exciton manifold by the photoluminescence.

The irreversible crossover is further confirmed from the von Neumann entropy $S(t) \equiv -\mathrm{Tr}[\hat{\rho}(t)\ln\hat{\rho}(t)]$. In Fig. 2(c), $S(t)$ initially remains small, which means that the initial dynamics is dominated by the time evolution of a quantum pure state. Then, the von Neumann entropy increases due to the decoherence by phonons, and shows two peaks approximately at 300 ps and 600 ns with strong mixing of states. These mixings, however, have different origins, i.e., the correlation between particles including quantum entanglement at ~300 ps and the classical stochastic mixing of the state at ~600 ns.

To distinguish these two distinct origins of the mixing, we introduce the quantum mutual information $I(t) \equiv S(\hat{\rho}(t)\|\hat{\rho}_X(t)\otimes\hat{\rho}_Y(t))$, where $S(\hat{\rho}\|\hat{\sigma}) \equiv \mathrm{Tr}[\hat{\rho}(\ln(\hat{\rho}) - \ln(\hat{\sigma}))]$ is the quantum relative entropy: a measure of the correlation between subsystems X and Y. We take X as the subsystem consisting of the photon and the bright exciton and take Y as the dark-exciton subsystem. Here, $\hat{\rho}_{X(Y)}(t)$ are the RDMs defined by the partial trace of the subsystem: $\hat{\rho}_{X(Y)}(t) \equiv \mathrm{Tr}_{Y(X)}[\hat{\rho}(t)]$.

While $I(t)$ is enhanced approximately at the first peak of $S(t)$, $t \simeq 300$ ps, it gives no peak at the second peak of $S(t)$, which suggests that the system becomes a nearly separable state with essentially no quantum entanglement after the first peak. Hence, the crossover occurs near the first peak. Ultimately, the fast relaxation from the bright exciton to the dark excitons and the rapid quantum-to-classical crossover do not contradict each other in the time domain.

Next, we examine the environmental effects on the time-resolved photoluminescence by monitoring κ as shown in Fig. 3(a). The photoluminescence decays are well fit by a triexponential function irrespective of κ though the decay constants strongly depend on κ. The fast and intermediate decay constants τ_1 and τ_2 are saturated with an increase in κ^{-1} as shown in Fig. 3(b). The positive correlation between τ_1 and τ_2 is clearly seen in Fig. 3(c), which is consistent with the experiment [23].

Finally, we emphasize the importance of the energy dissipation for the enhancement of the exciton lifetime.

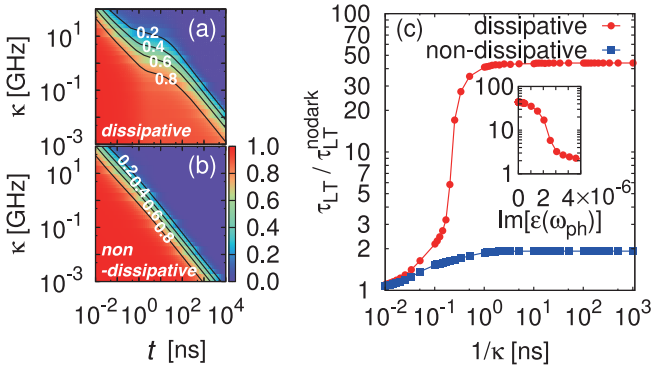

FIG. 4 (color online). (a),(b) Normalized energy $E/\varepsilon_{\rm br}$ as a function of time and κ for the (6,5) SWCNT model (dissipative system), and for the hypothetical model with the same parameters as those in the dissipative system except for the energy levels, $\hbar\omega_{\rm ph} = \varepsilon_{\rm br} = \varepsilon_{d1} = \varepsilon_{d2} = 1.27$ eV (nondissipative system). Solid lines indicate the contours of the normalized energy. (c) Energy lifetime $\tau_{\rm LT}$ as a function of κ in the dissipative and nondissipative systems. The lifetime is normalized by $\tau_{\rm TL}^{\rm nodark} = 2\kappa^{-1}$, which is the lifetime in the system with no dark exciton. The inset shows the normalized lifetime in the dissipative system as a function of $\mathrm{Im}[\varepsilon(\omega_{\rm ph})] = \kappa/\omega_{\rm ph}$.

Figures 4(a) and 4(b) show the system energy $E(t)$ as a function of time and κ for the systems where (a) the dark excitons have the lower energy compared to the bright one (dissipative system) or (b) all the excitons have the same energy level (nondissipative system). The energy $E(t)$ of the dissipative system obviously survives longer than that of the nondissipative system for small κ.

The difference is quantified in the lifetime $\tau_{\rm LT}$ as shown in Fig. 4(c). The lifetime in the dissipative system is about 45 times as long as $\tau_{\rm LT}^{\rm nodark}$ for large κ^{-1}. The large enhancement, which is not seen in the nondissipative system, suddenly occurs within a small range of κ. By relating κ to the background dielectric function $\varepsilon(\omega)$ with ω being a frequency using Poynting's theorem [56], $\kappa = \omega_{\rm ph}\mathrm{Im}[\varepsilon(\omega_{\rm ph})]$, the sudden enhancement of the lifetime is estimated to occur at $\mathrm{Im}[\varepsilon(\omega_{\rm ph})] \simeq 2\times10^{-6}$, which is comparable to that of water at room temperature, $\mathrm{Im}[\varepsilon(\omega_{\rm ph})] \simeq 1\times10^{-5}$ [57]. Therefore, the exciton lifetime of the SWCNT placed in the medium with smaller $\mathrm{Im}[\varepsilon(\omega_{\rm ph})]$, e.g., air, can be strongly enhanced.

In summary, we have investigated the effect of dissipation and decoherence on the long-term exciton dynamics in a model of the semiconducting (6,5) SWCNT. Counterintuitively, the dissipation and decoherence enhance the exciton lifetime in the relaxation pathway through the dark excitons, which paradoxically appears in experiments as a rapid decay of photoluminescence and a slow growth of quantum yield. In the search for efficient solar cells, such bad radiators are at first glance unpromising. However, we have shown this is not necessarily true. The present mechanism is generally applicable irrespective of material details if the relevant dark excitons exist. Indeed, semiconducting SWCNTs with various chirality are promising

materials that have relevant dark excitons and absorb the wide range of sunlight spectrum from infrared to visible light [38]. Therefore, our study confirms that semiconducting SWCNTs become potentially efficient photovoltaic materials, and provides a further guideline and insight into the high potentials of other unexplored materials with phosphorescence.

We acknowledge financial support by a Grant-in-Aid for Scientific Research (No. 22104010 and No. 22340090) from Ministry of Education, Culture, Sports, Science, and Technology (Japan), and a Grant-in-Aid for Scientific Research on Innovative Areas "Materials Design through Computics: Complex Correlation and Non-Equilibrium Dynamics." This work was also supported by MEXT HPCI Strategic Programs for Innovative Research (SPIRE) and RIKEN Advanced Institute for Computational Science (AICS) through the HPCI System Research Project (under Grants No. hp130007 and No. hp140215) and the Computational Materials Science Initiative (CMSI).

Note added.—Recently, a related paper appeared [58].

*Present address: Department of Physics, Osaka University, 1-1 Machikaneyama, Toyonaka, Osaka 560-0043, Japan.

[1] M. C. Beard, J. M. Luther, O. E. Semonin, and A. J. Nozik, Third generation photovoltaics based on multiple exciton generation in quantum confined semiconductors, Acc. Chem. Res. **46**, 1252 (2013).

[2] D. Jariwala, V. K. Sangwan, L. J. Lauhon, T. J. Marks, and M. C. Hersam, Carbon nanomaterials for electronics, optoelectronics, photovoltaics, and sensing, Chem. Soc. Rev. **42**, 2824 (2013).

[3] Q. H. Wang, K. Kalantar-zadeh, A. Kis, J. N. Coleman, and M. S. Strano, Electronics and optoelectronics of two-dimensional transition metal dichalcogenides, Nat. Nanotechnol. **7**, 699 (2012).

[4] W. H. Zurek, Decoherence, einselection, and the quantum origins of the classical, Rev. Mod. Phys. **75**, 715 (2003).

[5] G. D. Scholes, G. R. Fleming, A. Olaya-Castro, and R. van Grondelle, Lessons from nature about solar light harvesting, Nat. Chem. **3**, 763 (2011).

[6] R. E. Blankenship, D. M. Tiede, J. Barber, G. W. Brudvig, G. Fleming, M. Ghirardi, M. R. Gunner, W. Junge, D. M. Kramer, A. Melis *et al.*, Comparing photosynthetic and photovoltaic efficiencies and recognizing the potential for improvement, Science **332**, 805 (2011).

[7] C. A. Wraight and R. K. Clayton, The absolute quantum efficiency of bacteriochlorophyll photooxidation in reaction centres of Rhodopseudomonas spheroides, Biochim. Biophys. Acta **333**, 246 (1974).

[8] G. McDermott, S. M. Prince, A. A. Freer, A. M. Hawthornthwaite-Lawless, M. Z. Papiz, R. J. Cogdell, and N. W. Isaacs, Crystal structure of an integral membrane light-harvesting complex from photosynthetic bacteria, Nature (London) **374**, 517 (1995).

[9] H. Sumi, Theory on rates of excitation-energy transfer between molecular aggregates through distributed transition dipoles with application to the antenna system in bacterial photosynthesis, J. Phys. Chem. B **103**, 252 (1999).

[10] G. D. Scholes and G. R. Fleming, On the mechanism of light harvesting in photosynthetic purple bacteria: B800 to B850 energy transfer, J. Phys. Chem. B **104**, 1854 (2000).

[11] G. S. Engel, T. R. Calhoun, E. L. Read, T.-K. Ahn, T. Mančal, Y.-C. Cheng, R. E. Blankenship, and G. R. Fleming, Evidence for wavelike energy transfer through quantum coherence in photosynthetic systems, Nature (London) **446**, 782 (2007).

[12] P. Rebentrost, M. Mohseni, I. Kassal, S. Lloyd, and A. Aspuru-Guzik, Environment-assisted quantum transport, New J. Phys. **11**, 033003 (2009).

[13] M. B. Plenio and S. F. Huelga, Dephasing-assisted transport: quantum networks and biomolecules, New J. Phys. **10**, 113019 (2008).

[14] A. Ishizaki and G. R. Fleming, Unified treatment of quantum coherent and incoherent hopping dynamics in electronic energy transfer: Reduced hierarchy equation approach, J. Chem. Phys. **130**, 234111 (2009).

[15] E. Collini, C. Y. Wong, K. E. Wilk, P. M. G. Curmi, P. Brumer, and G. D. Scholes, Coherently wired light-harvesting in photosynthetic marine algae at ambient temperature, Nature (London) **463**, 644 (2010).

[16] K. E. Dorfman, D. V. Voronine, S. Mukamel, and M. O. Scully, Photosynthetic reaction center as a quantum heat engine, Proc. Natl. Acad. Sci. U.S.A. **110**, 2746 (2013).

[17] C. Creatore, M. A. Parker, S. Emmott, and A. W. Chin, Efficient Biologically Inspired Photocell Enhanced by Delocalized Quantum States, Phys. Rev. Lett. **111**, 253601 (2013).

[18] Y. Zhang, S. Oh, F. H. Alharbi, G. S. Engel, and S. Kais, Delocalized quantum states enhance photocell efficiency, Phys. Chem. Chem. Phys. **17**, 5743 (2015).

[19] F. Petruccione and H.-P. Breuer, *The theory of open quantum systems* (Oxford University Press, Berlin, 2002).

[20] M. D. Srinivas and E. B. Davies, Photon counting probabilities in quantum optics, Opt. Acta **28**, 981 (1981).

[21] M. D. Srinivas and E. B. Davies, What are the photon counting probabilities for open systems-a reply to Mandel's comments, Opt. Acta **29**, 235 (1982).

[22] S. Berciaud, L. Cognet, and B. Lounis, Luminescence Decay and the Absorption Cross Section of Individual Single-Walled Carbon Nanotubes, Phys. Rev. Lett. **101**, 077402 (2008).

[23] J. G. Duque, M. Pasquali, L. Cognet, and B. Lounis, Environmental and synthesis-dependent luminescence properties of individual single-walled carbon nanotubes, ACS Nano **3**, 2153 (2009).

[24] J. Park, P. Deria, and M. J. Therien, Dynamics and transient absorption spectral signatures of the single-wall carbon nanotube electronically excited triplet state, J. Am. Chem. Soc. **133**, 17156 (2011).

[25] D. Stich, F. Späth, H. Kraus, A. Sperlich, V. Dyakonov, and T. Hertel, Triplet–triplet exciton dynamics in single-walled carbon nanotubes, Nat. Photonics **8**, 139 (2014).

[26] H. Zhao and S. Mazumdar, Electron-Electron Interaction Effects on the Optical Excitations of Semiconducting

Single-Walled Carbon Nanotubes, Phys. Rev. Lett. **93**, 157402 (2004).
[27] C. D. Spataru, S. Ismail-Beigi, R. B. Capaz, and S. G. Louie, Theory and Ab Initio Calculation of Radiative Lifetime of Excitons in Semiconducting Carbon Nanotubes, Phys. Rev. Lett. **95**, 247402 (2005).
[28] T. Ando, Effects of valley mixing and exchange on excitons in carbon nanotubes with Aharonov–Bohm flux, J. Phys. Soc. Jpn. **75**, 024707 (2006).
[29] S. Tretiak, Triplet state absorption in carbon nanotubes: A TD–DFT study, Nano Lett. **7**, 2201 (2007).
[30] I. B. Mortimer and R. J. Nicholas, Role of Bright and Dark Excitons in the Temperature-Dependent Photoluminescence of Carbon Nanotubes, Phys. Rev. Lett. **98**, 027404 (2007).
[31] O. Kiowski, K. Arnold, S. Lebedkin, F. Hennrich, and M. M. Kappes, Direct Observation of Deep Excitonic States in the Photoluminescence Spectra of Single-Walled Carbon Nanotubes, Phys. Rev. Lett. **99**, 237402 (2007).
[32] J. Shaver, J. Kono, O. Portugall, V. Krstić, G. L. J. A. Rikken, Y. Miyauchi, S. Maruyama, and V. Perebeinos, Magnetic brightening of carbon nanotube photoluminescence through symmetry breaking, Nano Lett. **7**, 1851 (2007).
[33] R. Matsunaga, K. Matsuda, and Y. Kanemitsu, Evidence for Dark Excitons in a Single Carbon Nanotube due to the Aharonov-Bohm Effect, Phys. Rev. Lett. **101**, 147404 (2008).
[34] J. Shaver, S. A. Crooker, J. A. Fagan, E. K. Hobbie, N. Ubrig, O. Portugall, V. Perebeinos, P. Avouris, and J. Kono, Magneto-optical spectroscopy of highly aligned carbon nanotubes: Identifying the role of threading magnetic flux, Phys. Rev. B **78**, 081402 (2008).
[35] R. Matsunaga, K. Matsuda, and Y. Kanemitsu, Origin of low-energy photoluminescence peaks in single carbon nanotubes: K-momentum dark excitons and triplet dark excitons, Phys. Rev. B **81**, 033401 (2010).
[36] K. Nagatsu, S. Chiashi, S. Konabe, and Y. Homma, Brightening of Triplet Dark Excitons by Atomic Hydrogen Adsorption in Single-Walled Carbon Nanotubes Observed by Photoluminescence Spectroscopy, Phys. Rev. Lett. **105**, 157403 (2010).
[37] S. Konabe and K. Watanabe, Mechanism for optical activation of dark spin-triplet excitons in hydrogenated single-walled carbon nanotubes, Phys. Rev. B **83**, 045407 (2011).
[38] M. S. Arnold, J. L. Blackburn, J. J. Crochet, S. K. Doorn, J. G. Duque, A. Mohite, and H. Telg, Recent developments in the photophysics of single-walled carbon nanotubes for their use as active and passive material elements in thin film, Phys. Chem. Chem. Phys. **15**, 14896 (2013).
[39] See Supplemental Material at http://link.aps.org/supplemental/10.1103/PhysRevLett.115.197701 for a brief description of the method.
[40] T. Ogawa and T. Takagahara, Interband absorption spectra and Sommerfeld factors of a one-dimensional electron-hole system, Phys. Rev. B **43**, 14325 (1991).
[41] T. Ando, Excitons in carbon nanotubes, J. Phys. Soc. Jpn. **66**, 1066 (1997).
[42] F. Wang, G. Dukovic, L. E. Brus, and T. F. Heinz, The optical resonances in carbon nanotubes arise from excitons, Science **308**, 838 (2005).
[43] J. Kono, G. N. Ostojic, S. Zaric, M. S. Strano, V. C. Moore, J. Shaver, R. H. Hauge, and R. E. Smalley, Ultra-fast optical spectroscopy of micelle-suspended single-walled carbon nanotubes, Appl. Phys. A **78**, 1093 (2004).
[44] Y. Miyauchi, H. Hirori, K. Matsuda, and Y. Kanemitsu, Radiative lifetimes and coherence lengths of one-dimensional excitons in single-walled carbon nanotubes, Phys. Rev. B **80**, 081410 (2009).
[45] M. J. O'Connell, S. M. Bachilo, C. B. Huffman, V. C. Moore, M. S. Strano, E. H. Haroz, K. L. Rialon, P. J. Boul, W. H. Noon, C. Kittrell, J. Ma, R. H. Hauge, R. B. Weisman, and R. E. Smalley, Band gap fluorescence from individual single-walled carbon nanotubes, Science **297**, 593 (2002).
[46] Y. Piao, B. Meany, L. R. Powell, N. Valley, H. Kwon, G. C. Schatz, and Y. Wang, Brightening of carbon nanotube photoluminescence through the incorporation of sp^3 defects, Nat. Chem. **5**, 840 (2013).
[47] Y. Miyauchi, M. Iwamura, S. Mouri, T. Kawazoe, M. Ohtsu, and K. Matsuda, Brightening of excitons in carbon nanotubes on dimensionality modification, Nat. Photonics **7**, 715 (2013).
[48] V. Perebeinos and P. Avouris, Phonon and Electronic Nonradiative Decay Mechanisms of Excitons in Carbon Nanotubes, Phys. Rev. Lett. **101**, 057401 (2008).
[49] E. C. Sudarshan, P. M. Mathews, and J. Rau, Stochastic dynamics of quantum-mechanical systems, Phys. Rev. **121**, 920 (1961).
[50] E. B. Davies and J. T. Lewis, An operational approach to quantum probability, Commun. Math. Phys. **17**, 239 (1970).
[51] K. Kraus, General state changes in quantum theory, Ann. Phys. (N.Y.) **64**, 311 (1971).
[52] T. Arimitsu and H. Umezawa, Non-equilibrium thermo field dynamics, Prog. Theor. Phys. **77**, 32 (1987).
[53] M. Esposito, U. Harbola, and S. Mukamel, Nonequilibrium fluctuations, fluctuation theorems, and counting statistics in quantum systems, Rev. Mod. Phys. **81**, 1665 (2009).
[54] M. S. Dresselhaus and P. C. Eklund, Phonons in carbon nanotubes, Adv. Phys. **49**, 705 (2000).
[55] T. B. Norris, J. K. Rhee, C. Y. Sung, Y. Arakawa, M. Nishioka, and C. Weisbuch, Time-resolved vacuum Rabi oscillations in a semiconductor quantum microcavity, Phys. Rev. B **50**, 14663 (1994).
[56] J. D. Jackson, *Classical Electrodynamics*, 3rd ed. (Wiley, New York, 1999).
[57] K. F. Palmer and D. Williams, Optical properties of water in the near infrared, J. Opt. Soc. Am. **64**, 1107 (1974).
[58] S. Ajisaka, B. Źunković, and Y. Dubi, The molecular photocell: quantum transport and energy conversion at strong non-equilibrium, Sci. Rep. **5**, 8312 (2015).